

## Surface critical behavior of driven diffusive systems with open boundaries

K. Oerding and H. K. Janssen

*Institut für Theoretische Physik III, Heinrich-Heine-Universität, D-40225 Düsseldorf, Germany*

(Received 17 February 1998)

Using field theoretic renormalization group methods we study the critical behavior of a driven diffusive system near a boundary perpendicular to the driving force. The boundary acts as a particle reservoir, which is necessary to maintain the critical particle density in the bulk. The scaling behavior of correlation and response functions is governed by a new exponent  $\eta_1$ , which is related to the anomalous scaling dimension of the chemical potential of the boundary. The new exponent and a universal amplitude ratio for the density profile are calculated at first order in  $\epsilon = 5 - d$ . Some of our results are checked by computer simulations. [S1063-651X(98)04308-6]

PACS number(s): 05.40.+j, 05.70.Fh, 64.60.Ak, 66.30.Dn

### I. INTRODUCTION

In order to study the properties of thermodynamic systems far from equilibrium physicists have been looking for simple models that capture the main features of nonequilibrium phenomena. Driven diffusive systems (DDS) introduced by Katz *et al.* [1] to model fast ionic conductors are characterized by a particle conserving dynamics and a stationary state, which does not satisfy detailed balance. Their study has led to the discovery of the connection between the validity of a conservation law and the existence of long-range spatial correlations in nonequilibrium steady states.

A simple microscopic realization of DDS is an Ising lattice gas with attractive nearest neighbor interaction and an external driving force  $E$  that prefers particle jumps in the direction parallel to  $E$  [1,2]. The strength of the particle attraction can be varied by a temperaturelike parameter  $T$ . Below a critical value  $T_c(E)$  particles are separated in the stationary state into regions of high and low densities, where the interfaces are oriented parallel to the driving force (for  $E \neq 0$ ). The phase transition at  $T_c(E)$  is second order. For an infinite driving force particle jumps in the direction antiparallel to  $E$  are suppressed. In this case the phase transition occurs at  $T_c(\infty) \approx 1.41T_c(0)$ , where  $T_c(0)$  is the critical temperature of the two dimensional Ising model [2]. The critical behavior of this system has been extensively studied by Monte Carlo simulations and renormalization group methods [3]. (For a recent review see [4].)

In most studies of DDS periodic boundary conditions in all directions are imposed to avoid surface effects. In this case the particles are driven along a ring or torus. In more realistic models particles are fed into the system at one side and extracted at the other. The asymmetric exclusion model [5] is a DDS with hard core repulsion (but without nearest neighbor interaction, i.e.,  $T = \infty$ ). The density profile in a one-dimensional exclusion model with a particle source and a sink was investigated numerically by Krug [6]. His results were later confirmed and generalized by exact calculations [7–9]. An important result of these works is the “maximum current principle,” which states the following: If the system is placed between two particle reservoirs  $A$  and  $B$  (with the respective densities  $c_A$  and  $c_B$  with  $c_A \geq c_B$ ) and the driving force points from  $A$  to  $B$ , then the bulk density takes the

value  $c_{\max}$ , which maximizes the current  $j$  under the constraint  $c_A \geq c \geq c_B$ , i.e.,

$$j(c_{\max}) = \max\{j(c) | c_A \geq c \geq c_B\}. \quad (1)$$

The maximum current density of an Ising lattice gas with attractive particle-particle interaction equals its critical density  $1/2$ . The low temperature phase of this system with open boundaries in two dimensions has been studied by Boal *et al.* [10].

In the present paper field theoretic renormalization group methods are employed to investigate the effects of open boundaries on DDS at the critical point  $T_c(E)$ . We assume that a plane particle source  $A$  perpendicular to the driving force is located at the left boundary of the system (coordinate  $z=0$ ) and impose periodic boundary conditions in the transverse directions. The effect of the particle source is to suppress density fluctuations and to maintain a constant density  $c_A$  at  $z=0$ . The particles are extracted from the system when they reach a sink  $B$  located at  $z=L$  ( $L \rightarrow \infty$ ).

It is well known that in physical systems with long ranged correlations the influence of a surface extends far into the bulk. The critical behavior near a boundary is governed by universal scaling laws with critical exponents that (in general) cannot be expressed in terms of bulk exponents (a review is given in Ref. [11]). The applicability of renormalization group methods to investigate both static [11–15] and dynamic [16–18] surface universality classes is well established. Especially encouraging are the results of Ref. [19] where this technique has been used to obtain an approximate profile for one-dimensional DDS with open boundaries. It turned out that the profile calculated by renormalization group improved perturbation theory (at one-loop order) was in good agreement with the exact result of Ref. [7].

In the next section the semi-infinite extension of the field theoretic model for DDS at the critical point (introduced in [3]) is presented. Above the upper critical dimension  $d_c = 5$  of this model fluctuations around the mean field profile can be treated by naive perturbation theory. The mean field profile and Gaussian fluctuations for  $d > 5$  are considered in some detail in Secs. III and IV since the results of this analysis remain qualitatively valid for  $d < 5$ . In Sec. V the renormalization group is used to obtain the scaling behavior of

Green functions and the density profile below five dimensions. Section VII contains a discussion.

## II. MODEL

The analysis in the present paper is based on the field theoretic model introduced by Janssen and Schmittmann [3] to study the critical behavior of a diffusive system with a single conserved density subjected to an external driving force. The model can be written in the form of the continuity equation

$$\partial_t s + \nabla_{\perp} \cdot \mathbf{j}_{\perp} + \partial_{\parallel} j_{\parallel} = 0, \quad (2)$$

where  $s(\mathbf{r}, t) = c(\mathbf{r}, t) - \bar{c}$  denotes the deviation of the concentration from its average (bulk) value  $\bar{c}$ , and  $\mathbf{j}_{\perp}$  and  $j_{\parallel}$  are the respective components of the current perpendicular and parallel to the driving force. The explicit expression for the current can be motivated by the following symmetry requirements [4]: (i) isotropy with respect to the  $(d-1)$ -dimensional transverse subspace, (ii) invariance of the equation of motion under reversal of the driving force ( $E \leftrightarrow -E$ ) and particle-hole exchange (“charge conjugation,”  $s \leftrightarrow -s$ ), (iii) invariance under force reversal and reflection in  $r_{\parallel}$  (the coordinate parallel to the force). A continuum model satisfying (i)–(iii) describes, for instance, the long time and large distance behavior of a driven Ising lattice gas at its critical density  $1/2$ . Since the current in this system is at its maximum value for half filling one may use the maximum current principle (in a system with open boundaries) to adjust the bulk density to the critical value.

Keeping only terms that are consistent with the above conditions (i)–(iii) and relevant or marginal in the renormalization group sense the current may be written (upon rescaling of  $s$ ) in the form

$$j_{\perp} = \nabla_{\perp} [-\lambda(\tau s - \Delta_{\perp} s) + \zeta], \quad (3a)$$

$$j_{\parallel} = E(\sigma_0 + \sigma_2 s^2) - \lambda \rho \partial_{\parallel} s, \quad (3b)$$

where  $\zeta$  is a Gaussian random force with the correlation

$$\langle \zeta(\mathbf{r}, t) \zeta(\mathbf{r}', t') \rangle = 2\lambda \delta(\mathbf{r} - \mathbf{r}') \delta(t - t'). \quad (3c)$$

The third order derivative in Eq. (3a) has to be kept because the coefficient  $\tau$  of the first order derivative vanishes at the critical point (transverse phase transition [3]). The coefficient  $\sigma_0$  may be interpreted as the conductivity of the system at the maximum current density  $\bar{c}$ . Deviations from  $\bar{c}$  due to fluctuations or a nonconstant density profile decrease the current. This effect is modeled by the term  $E\sigma_2 s^2$  in Eq. (3b). The coefficient  $\tau$  measures the deviation of the temperature parameter from its critical value and  $\rho$  takes into account the anisotropy of the diffusion constant. Even if the diffusion constant is isotropic ( $\rho = 1$ ) in the original Langevin equation it becomes anisotropic under coarse graining.

For the subsequent field theoretic analysis it is convenient to recast the model in the form of the dynamic functional [20–24,3]

$$\begin{aligned} \mathcal{J}_b[\tilde{s}, s] = & \int dt \int_V d^d r \{ \tilde{s} \partial_t s + \lambda [(\Delta_{\perp} \tilde{s})(\Delta_{\perp} s) \\ & + \tau(\nabla_{\perp} \tilde{s})(\nabla_{\perp} s) + \rho(\partial_{\parallel} \tilde{s})(\partial_{\parallel} s) \\ & + \frac{1}{2} g(\partial_{\parallel} \tilde{s})s^2 - h \partial_{\parallel} \tilde{s} - (\nabla_{\perp} \tilde{s})^2 \}, \end{aligned} \quad (4)$$

where  $\lambda g \sim -E\sigma_2$ , and  $\tilde{s}$  is a Martin-Siggia-Rose response field [25]. While the functional (4) allows us to calculate response and correlation functions for an infinite bulk system the influence of the boundaries has to be modeled by additional surface contributions. If the boundary is perpendicular to the driving force the region of integration in Eq. (4) is the half space  $V = \{(\mathbf{r}_{\perp}, z) | \mathbf{r}_{\perp} \in \mathbb{R}^{d-1}, z \geq 0\}$ , and the surface is defined by  $z = 0$ . Omitting irrelevant and redundant terms [19] the surface functional reads

$$\begin{aligned} \mathcal{J}_s[\tilde{s}, s] = & \int dt \int_{\partial V} d^{d-1} r_{\perp} \lambda \\ & \times (c \tilde{s} s - \tilde{c} \tilde{s}^2 - c_2 \tilde{s} \Delta_{\perp} s + \frac{1}{2} g_s \tilde{s} s^2 - h_s \tilde{s}). \end{aligned} \quad (5)$$

Response and correlation functions can now be calculated by functional integration with the weight  $\exp(-\mathcal{J})$ , where  $\mathcal{J} = \mathcal{J}_b + \mathcal{J}_s$ .

## III. EQUATION OF MOTION AND MEAN FIELD APPROXIMATION

An exact equation for the stationary profile  $\Phi(z) = \langle s(\mathbf{r}, t) \rangle$  follows from the invariance of the generating functional

$$\begin{aligned} Z[\tilde{J}, J; \tilde{J}_1, J_1] = & \int \mathcal{D}[\tilde{s}, s] \exp[-\mathcal{J}_b[\tilde{s}, s] - \mathcal{J}_s[\tilde{s}, s, s_s] + (\tilde{J}, \tilde{s}) \\ & + (J, s) + (\tilde{J}_1, \tilde{s}_s) + (J_1, s_s)] \end{aligned} \quad (6)$$

under an infinitesimal shift of the field  $\tilde{s}$ . In Eq. (6)  $s_s(\mathbf{r}_{\perp}) = s(\mathbf{r}_{\perp}, 0)$  denotes the field at the surface and the abbreviations

$$(\tilde{J}, \tilde{s}) = \int dt \int_V d^d r \tilde{J} \tilde{s} \quad (7)$$

and

$$(J_1, s_s) = \int dt \int_{\partial V} d^{d-1} r_{\perp} J_1 s_s \quad (8)$$

have been used. The invariance of  $Z[\tilde{J}, J; \tilde{J}_1, J_1]$  implies the equation of motion

$$\partial_t s + \lambda [(\Delta_{\perp} - \tau) \Delta_{\perp} s - \partial_{\parallel} (\rho \partial_{\parallel} s + \frac{1}{2} g s^2) + 2 \Delta_{\perp} \tilde{s}] = \tilde{J}, \quad (9)$$

which holds after insertion into averages. The invariance of  $Z[\tilde{J}, J; \tilde{J}_1, J_1]$  under a shift of the surface field  $\tilde{s}_s$  leads to the equation of motion

$$-\rho\partial_n s - \frac{g^- g_s}{2} s_s^2 + c s_s - 2\tilde{c} s_s - c_2 \Delta_\perp s_s - h_s + h = \frac{1}{\lambda} \tilde{J}_1, \quad (10)$$

which fixes the boundary condition. Taking the average on both sides of Eq. (9) for vanishing sources  $\tilde{J} = J = \tilde{J}_1 = J_1 = 0$  one obtains

$$\partial_z \{ \rho \partial_z \Phi(z) + \frac{1}{2} g [\Phi(z)^2 + C(z)] \} = 0 \quad (11)$$

or, since  $\Phi_{\text{bulk}} = 0$  due to the definition of  $s$ ,

$$\Phi'(z) + \frac{g}{2\rho} [\Phi(z)^2 + C(z) - C_{\text{bulk}}] = 0. \quad (12)$$

The function  $C(z) = \langle [s(\mathbf{r}_\perp, z; t) - \Phi(z)]^2 \rangle$  describes density fluctuations at the distance  $z$  from the surface and  $C_{\text{bulk}}$  denotes its value for  $z \rightarrow \infty$ .

In the mean field approximation one neglects the correlation function  $C(z)$  and obtains for the profile

$$\Phi_{\text{mf}}(z) = \Phi_0 \left( 1 + \frac{g}{2\rho} \Phi_0 z \right)^{-1}. \quad (13)$$

Dimensional analysis shows that the momentum dimension of the coupling coefficient  $g$  is given by  $[g] = (5-d)/2$ , and the mean field approximation breaks down below the upper critical dimension  $d_c = 5$ . For  $d > 5$  corrections to the mean field profile can be obtained by naïve perturbation theory. At lowest order it is sufficient to calculate the perturbation  $C(z) - C_{\text{bulk}}$  in Eq. (12) by a Gaussian approximation.

#### IV. CORRECTIONS TO THE MEAN FIELD PROFILE FOR $d > 5$

In the simplest case,  $\Phi_{\text{mf}}(z) = \Phi_0 = h_s = 0$ , the Fourier transform (with respect to  $\mathbf{r}_\perp$  and  $t$ ) of the Gaussian propagator

$$G(\mathbf{r}_\perp, z, z'; t) = \langle s(\mathbf{r}_\perp, z; t) \tilde{s}(\mathbf{0}, z'; 0) \rangle_0 \quad (14)$$

is given by [19]

$$\hat{G}_{\mathbf{q}_\perp, \omega}(z, z') = \frac{1}{2\lambda\sqrt{\rho}\kappa} \left[ e^{-\kappa|z-z'|/\sqrt{\rho}} + \frac{\kappa - c/\sqrt{\rho}}{\kappa + c/\sqrt{\rho}} e^{-\kappa(z+z')/\sqrt{\rho}} \right] \quad (15)$$

with

$$\kappa = \left( \frac{i\omega}{\lambda} + q_\perp^2(\tau + q_\perp^2) \right)^{1/2}. \quad (16)$$

The parameter  $c$  occurring in the surface functional  $\mathcal{J}_1$  and in the propagator describes (for  $c > 0$ ) the suppression of density fluctuations by the particle reservoir at the boundary. Since the momentum dimension of  $c$  is one the asymptotic scaling behavior is governed by the fixed point  $c_\star = \infty$ . At this fixed point the fields  $\tilde{s}$  and  $s$  satisfy the Dirichlet boundary conditions  $\tilde{s}_s = s_s = 0$ .

The Fourier transform of the Gaussian correlation function

$$C(\mathbf{r}_\perp, z, z'; t) = \langle s(\mathbf{r}_\perp, z; t) s(\mathbf{0}, z'; 0) \rangle_0 \quad (17)$$

at the Dirichlet fixed point  $c_\star = \infty$  can be derived from the Gaussian part of the dynamic functional. This calculation yields

$$\begin{aligned} \hat{C}_{\mathbf{q}_\perp, \omega}(z, z') &= 2\lambda q_\perp^2 \int_0^\infty dz'' \hat{G}_{\mathbf{q}_\perp, \omega}(z, z'') \hat{G}_{\mathbf{q}_\perp, -\omega}(z'', z') \\ &= -\frac{2\lambda q_\perp^2}{\omega} \text{Im}[\hat{G}_{\mathbf{q}_\perp, \omega}(z, z')], \end{aligned} \quad (18)$$

where  $\text{Im}[\dots]$  denotes the imaginary part. The equal-time correlation function at the point  $(\mathbf{r}_\perp, z)$  is given by

$$\begin{aligned} C(z) &= \int_{\mathbf{q}_\perp, \omega} \hat{C}_{\mathbf{q}_\perp, \omega}(z, z) \\ &= C_{\text{bulk}} - \frac{1}{2\sqrt{\rho}} (8\pi z/\sqrt{\rho})^{-(d-1)/2} \end{aligned} \quad (19)$$

with  $C_{\text{bulk}} \sim \Lambda^{d-1}/\sqrt{\rho}$  (where  $\Lambda$  is a cutoff wave number).

We can now use Eqs. (12) and (19) to compute the fluctuation correction to the constant mean field profile  $\Phi_{\text{mf}}(z) = 0$ . At first order in  $g$  we get

$$\Phi^{(1)}(z) = -\frac{g(8\pi)^{-(d-1)/2}}{2(d-3)\rho} \left( \frac{z}{\sqrt{\rho}} \right)^{-(d-3)/2}. \quad (20)$$

One can easily check by dimensional analysis that higher order corrections to the profile decay as  $\Phi^{[2n+1]}(z)/\Phi^{[1]}(z) \sim z^{-n(d-5)/2}$  (up to cutoff dependent terms, which may change the amplitude of the leading term proportional to  $z^{-(d-3)/2}$ ).

In the limit  $c, h_s \rightarrow \infty$  (with  $h_s/c =: h_1$  fixed) the boundary value of the mean field profile is given by  $\Phi_0 = h_1$ . This follows from Eqs. (10) and (13). For  $\Phi_0 > 0$  the mean field profile decays asymptotically as  $\Phi_{\text{mf}}(z) \approx 2\rho/(gz)$ , and the fluctuation correction  $\sim z^{-(d-3)/2}$  can be neglected for  $z \rightarrow \infty$  ( $d > 5$ ). However, if  $h_1$  is positive but small the profile  $\Phi(z)$  is negative for  $z < \zeta$ , where  $\zeta = \zeta(h_1)$  is a crossover length. The dependence of the profile on the boundary chemical potential  $h_1$  is depicted qualitatively in Fig. 1. The crossover length  $\zeta$  tends to infinity for  $h_1 \rightarrow 0^+$ . To estimate  $\zeta$  for small  $h_1$  we equate the mean field profile  $\Phi_{\text{mf}}(\zeta)$  with the fluctuation term  $\zeta^{-(d-3)/2}$  and obtain

$$\zeta \sim h_1^{-2/(d-3)} \quad (21)$$

for  $h_1 \rightarrow 0^+$ ,  $d > 5$ .

In the language of semi-infinite magnetic systems the case  $h_1 = \infty$  corresponds to the normal transition and  $h_1 = 0$  is the ordinary point. A length scale similar to  $\zeta$  has already been found in magnetic systems at the ordinary transition [26]. There the length scale  $\zeta$  characterizes the magnetization profile induced by a small magnetic surface field.

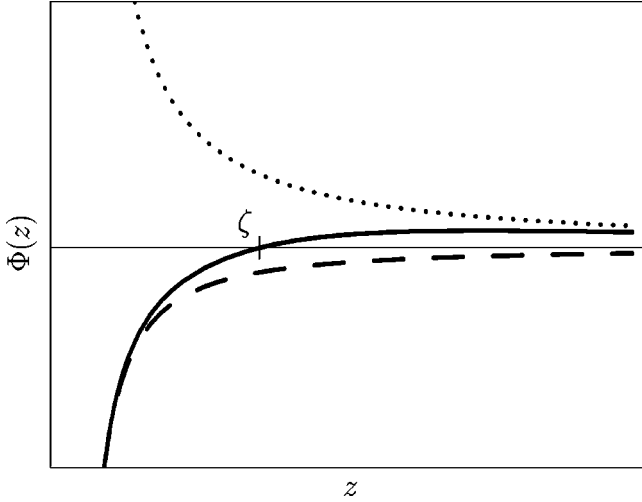


FIG. 1. Sketch of the profile  $\Phi(z)$  for  $h_1 = \infty$  (dotted),  $h_1 > 0$  finite (solid curve), and  $h_1 = 0$  (dashed). For  $h_1 < 0$  the density in the bulk stays below its critical value indicated by the horizontal line.

## V. RENORMALIZATION GROUP ANALYSIS

### A. Renormalization

The naive perturbation theory described in the previous section breaks down below the upper critical dimension  $d_c = 5$ . The renormalization group allows us to improve the perturbation expansion by a partial resummation.

Since the individual terms of the perturbation series contain for  $d = d_c$  ultraviolet divergent integrals a regularization prescription is required to obtain well-defined expressions for the otherwise infinite integrals. Here we use the dimensional regularization method (analytic continuation of the integrals as functions of  $d$ ). The remaining poles in  $\epsilon = d_c - d$  are then absorbed into reparametrizations of the coupling coefficients and the fields. In the field theory for the bulk model (without a surface) a renormalization of the parameter  $\rho = Z\rho_R$  is sufficient to cancel the ultraviolet divergences at every order of the perturbation theory [3]. At one-loop order the renormalization factor is given by

$$Z = 1 - \frac{u}{\epsilon} + O(u^2), \quad u = A_\epsilon g^2 \rho_R^{-3/2} \mu^{-\epsilon}, \quad (22)$$

where  $\mu$  is an external momentum scale and the geometrical factor  $A_\epsilon = (3/4)(4\pi)^{-d/2} \Gamma[(3-\epsilon)/2] \Gamma(1+\epsilon/2) / \Gamma(2-\epsilon/2)$  has been introduced for convenience. (The index  $R$  indicates renormalized quantities.)

In order to investigate the scaling behavior of response functions near the boundary one has to calculate Green functions with insertions of the surface response field  $\tilde{s}_s$ . Since the Gaussian propagator (15) vanishes at the Dirichlet fixed point  $c_* = \infty$  it is necessary to go to higher orders in  $c^{-1}$  to obtain nontrivial results [11,12,27]. At first order in  $c^{-1}$  the propagator becomes (for  $z' = 0$ )

$$\hat{G}_{\mathbf{q}_\perp, \omega}(z, 0) = \frac{1}{c} \rho \partial_z \hat{G}_{\mathbf{q}_\perp, \omega}^{(D)}(z, z')|_{z'=0} + \dots, \quad (23)$$

where  $\hat{G}_{\mathbf{q}_\perp, \omega}^{(D)}(z, z')$  denotes the propagator (15) for  $c = \infty$ . This shows that the leading order terms in an expansion in powers of  $c^{-1}$  can be studied in the framework of a field theory with Dirichlet boundary conditions after replacing in expectation values

$$\tilde{s}_s \rightarrow c^{-1} \rho \partial_n \tilde{s}. \quad (24)$$

Analogously insertions of the surface field  $s_s$  have to be replaced (at leading order) by the normal derivative  $c^{-1} \rho \partial_n s$ .

Since a boundary breaks the translational invariance of the system it gives rise to new divergences in the perturbation series that are located at the surface [i.e., proportional to  $\delta(z)$ ]. These surface divergences have to be subtracted by appropriate counter terms added to the dynamic functional  $\mathcal{J}$ . In the Appendix it is shown that the required counter terms have the form

$$\begin{aligned} \mathcal{J}_{\text{bct}}[\tilde{s}, s] = & \int dt \int_V d^d r \lambda [\rho_R (Z-1) (\partial_\parallel \tilde{s}) (\partial_\parallel s) \\ & + \rho_R^{-1/2} A_\epsilon g \mu^{-\epsilon} A \tau^2 \partial_\parallel \tilde{s}] \end{aligned} \quad (25)$$

to remove bulk divergences and

$$\begin{aligned} \mathcal{J}_{\text{scf}}[\tilde{s}, s] = & \int dt \int_{\partial V} d^{d-1} r_\perp \lambda [\rho_R^{-1/2} A_\epsilon g \mu^{-\epsilon} K (\rho \partial_n^2 \tilde{s}) \\ & + B (\rho \partial_n \tilde{s}) s_s + \rho_R^{-1} A_\epsilon g \mu^{-\epsilon} F \tau (\rho \partial_n \tilde{s})] \end{aligned} \quad (26)$$

to cancel  $\epsilon$  poles located at the surface. The renormalization parameters  $A, B, F, K$  are calculated at one-loop order with the result

$$A = -\frac{1}{\epsilon}, \quad B = -\frac{u}{3\epsilon}, \quad F = -\frac{4}{3\epsilon}, \quad K = \frac{2}{3\epsilon}. \quad (27)$$

The first term in  $\mathcal{J}_{\text{bct}}$  renormalizes the diffusion coefficient  $\rho$ . The bulk counterterm proportional to  $\partial_\parallel \tilde{s}$  corresponds to a renormalization of the bulk current [28]

$$h = h_R - \rho_R^{-1/2} A_\epsilon g \mu^{-\epsilon} A \tau^2. \quad (28)$$

The surface counterterms proportional to the redundant operators  $(\rho \partial_n \tilde{s}) s_s$  and  $\rho \partial_n^2 \tilde{s}$  are equivalent to a multiplicative renormalization of the surface response field  $\rho \partial_n \tilde{s}$ ,

$$[\rho \partial_n \tilde{s}]_R = Z_1^{-1/2} \rho \partial_n \tilde{s}. \quad (29)$$

For the semi-infinite  $\phi^4$  model (where the counterterm  $\rho \partial_n^2 \tilde{s}$  is absent) this has been shown in Ref. [29]. In the present case both counterterms contribute to the renormalization factor  $Z_1$ . In Fig. 2 it is shown that an insertion of the operator  $\rho \partial_n^2 \tilde{s}$  into a Feynman diagram has the same effect as  $(\rho \partial_n \tilde{s}) s_s$ .

At one-loop order one gets

$$Z_1^{-1/2} = 1 - B - uK + O(u^2) = 1 - \frac{u}{3\epsilon} + O(u^2). \quad (30)$$

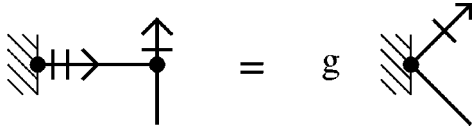


FIG. 2. Effect of the vertex  $\lambda \rho \partial_n^2 \tilde{s}$  in a Feynman diagram. The hatched area represents the boundary  $z=0$ . Each short line perpendicular to a propagator line indicates a derivative with respect to  $z$ .

The relation between the redundant surface couplings (here  $B$ ,  $K$ ) and  $Z_1$  can be extended to higher orders in  $u$  in a similar way as in Ref. [29]. The last counter term in  $\mathcal{J}_{\text{set}}$  that couples to  $\rho \partial_n \tilde{s}$  renormalizes the surface chemical potential

$$h_1 = Z_1^{-1/2} ([h_1]_R - \rho_R^{-1} A_\epsilon g \mu^{-\epsilon} F \tau). \quad (31)$$

### B. Scaling

With the renormalizations at hand we are in a position to determine the scaling behavior of Green functions and the density profile. For this purpose we need the anomalous momentum dimensions of the fields and coupling coefficients. At the fixed point  $u_* = (2/3)\epsilon + O(\epsilon^2)$  of the renormalization group the couplings  $\rho$  and  $h_1$  scale as

$$\rho \sim l^{-2\eta}, \quad h_1 \sim \rho^{-1/4} l^{(d-1-\eta_1)/2} \sim l^{(d-1+\eta-\eta_1)/2}, \quad (32)$$

where  $l$  is a flow parameter and  $\eta$  and  $\eta_1$  are the respective fixed point values of the Wilson functions

$$\gamma(u) = -\frac{1}{2} \mu \left. \frac{d \ln \rho}{d \mu} \right|_0 = \frac{1}{2} u + O(u^2), \quad (33a)$$

$$\gamma_1(u) = \mu \left. \frac{d \ln Z_1}{d \mu} \right|_0 = -\frac{2}{3} u + O(u^2). \quad (33b)$$

The derivatives are calculated at fixed bare parameters. From this one finds

$$\eta = \frac{5-d}{3}, \quad \eta_1 = -\frac{4\epsilon}{9} + O(\epsilon^2), \quad (34)$$

where the expression for  $\eta$  holds at every order of the  $\epsilon$  expansion [3]. The scaling dimensions of the coordinates  $r_\perp \sim l^{-1}$ ,  $r_\parallel \sim \rho^{1/2} l^{-2} \sim l^{-(2+\eta)}$  and the bulk fields  $\tilde{s} \sim \rho^{-1/4} l^{(d+3)/2} \sim l^{(d+3+\eta)/2}$ ,  $s \sim \rho^{-1/4} l^{(d-1)/2} \sim l^{(d-1+\eta)/2}$  may also be derived from the renormalization group equations [3,4].

The scaling form of the density profile for  $\tau = h = 0$  now follows from dimensional analysis (using instead of the naive momentum dimensions the anomalous dimensions given above) as

$$\Phi(z, h_1) = a z^{-\sigma} F(b h_1 z^{1/\nu_1}), \quad (35)$$

with the exponents

$$\sigma = \frac{d-1+\eta}{2(2+\eta)} = \frac{1+d}{11-d} \quad (36)$$

and

$$\frac{1}{\nu_1} = \frac{d-1+\eta-\eta_1}{2(2+\eta)} = 1 - \frac{2\epsilon}{9} + O(\epsilon^2). \quad (37)$$

In Eq. (35)  $a$  and  $b$  are nonuniversal scale factors while the scaling function  $F$  is universal.

### C. Universal amplitude ratio

We know from the discussion of the mean field profile and the fluctuation corrections in Sec. IV that  $\Phi(z, h_1)$  is finite and nonzero in both cases  $h_1 = \infty$  and  $h_1 = 0$ . It therefore makes sense to define the universal amplitude ratio

$$D = \lim_{z \rightarrow \infty} \frac{\Phi(z, 0)}{\Phi(z, \infty)} = \frac{F(0)}{F(\infty)}. \quad (38)$$

A perturbative calculation based on the results of Sec. IV yields

$$\begin{aligned} \frac{\Phi(z, 0)}{\Phi(z, \infty)} &= -\frac{g^2 (8\pi)^{-(d-1)/2}}{4(d-3)\rho^{3/2}} \left( \frac{z}{\sqrt{\rho}} \right)^{\epsilon/2} + O(g^4) \\ &= -\frac{u}{6} + O(u^2, u\epsilon). \end{aligned} \quad (39)$$

At the fixed point of the renormalization group this becomes

$$D = -\frac{\epsilon}{9} + O(\epsilon^2). \quad (40)$$

In the upper critical dimension  $d=5$  the coupling coefficient  $u$  tends to zero under application of the renormalization group. The solution of the renormalization group equations as in Ref. [19] yields

$$\bar{u}(l) \approx \frac{2}{3 \ln(1/l)} \quad \text{for } l \rightarrow 0. \quad (41)$$

This gives for the profile

$$\frac{\Phi(z, 0)}{\Phi(z, \infty)} \approx -\frac{2}{9 \ln(z/z_0)} \quad \text{for } z \rightarrow \infty, \quad (42)$$

where  $z_0$  is nonuniversal.

Above five dimensions the amplitude ratio vanishes. The reason is that the coupling  $g$ , which is dangerously irrelevant for  $d \geq 5$ , enters the profile for  $h_1 = 0$  and  $h_1 = \infty$  in different ways. Since  $g$  is responsible for the coupling between the average density and density correlations [see Eq. (12)] the modulus of the profile for  $h_1 = 0$  is an increasing function of  $g$ . For  $h_1 = \infty$ , on the other hand, the profile is a decreasing function of  $g$  [see Eq. (13)]. In this case the main effect of  $g$  is to suppress deviations from the maximum current density  $\bar{c}$  in the bulk. Since the ratio  $\Phi(z, 0)/\Phi(z, \infty)$  is for large  $z$  proportional to a positive power of  $g$  and  $g$  is irrelevant for  $d \geq 5$  the ratio tends to zero for  $z \rightarrow \infty$ . For  $d < 5$  the renormalized counterpart of  $g$  tends to a positive fixed point value giving rise to a nonzero value of  $D$ .

### D. Distant wall corrections

Until now the profile near a particle source has been investigated assuming that the particles are extracted by a distant sink located at  $z=L$ ,  $L \rightarrow \infty$ . In computer simulations only comparatively small systems can be studied and corrections to the profile (35) due to the distant sink become important. At mean field level the profile that satisfies the boundary conditions  $\Phi(0)=\infty$  and  $\Phi(L)=-\infty$  is given by

$$\Phi_{\text{mf}}(z) = \frac{2\pi\rho}{gL} \cot\left(\frac{\pi z}{L}\right) = \frac{2\rho}{gz} \left[ 1 - \frac{1}{3} \left(\frac{\pi z}{L}\right)^2 + \dots \right]. \quad (43)$$

The powers of  $(z/L)$  occurring in this expansion below the upper critical dimension can be obtained from a short distance expansion (SDE) of the order parameter field  $s(z)$  for  $z \rightarrow 0$  [31–33]. The leading term in this SDE (with the lowest momentum dimension) is the unit operator 1. Since  $s_s=0$  due to the Dirichlet boundary condition the next-to-leading contribution is the normal derivative  $\rho \partial_n s$ . We therefore obtain

$$s(r_\perp, z, t) = A_1 z^{-\sigma} \times 1 + A_2 z^{(2-\eta)/(2+\eta)} \rho \partial_n s(r_\perp, t) + \dots \quad (44)$$

The power in front of the normal derivative has been determined by comparing the anomalous scaling dimensions of the individual terms in Eq. (44),

$$s \sim l^{(d-1+\eta)/2}, \quad \rho \partial_n s \sim l^{(d+3-\eta)/2}, \quad z \sim l^{-(2+\eta)}. \quad (45)$$

The SDE (44) implies that the distant particle sink gives rise to a correction to the profile proportional to  $z^{(2-\eta)/(2+\eta)} = z^\sigma$  for  $z \rightarrow 0$ , i.e.,

$$\Phi(z) = A_1 z^{-\sigma} \left[ 1 + B \left(\frac{z}{L}\right)^{2\sigma} + \dots \right]. \quad (46)$$

For  $\epsilon=0$  this form is consistent with the mean field result (43).

The amplitudes  $A_1$  and  $B$  depend on the fixed point value of the surface potential, i.e., they take different values for  $h_1=0$  and  $h_1=\infty$ . Equation (43) shows that for  $h_1=\infty$  the (universal) amplitude  $B$  is given by  $B = -\pi^2/3 + O(\epsilon)$ . In the case  $h_1=0$  with the boundary conditions  $\Phi_{\text{mf}}(0)=0$  and  $\Phi(L)=-\infty$  the mean field profile reads

$$\Phi_{\text{mf}}(z) = -\frac{\pi\rho}{gL} \tan\left(\frac{\pi z}{2L}\right) = -\frac{\pi^2\rho}{2gz} \left[ \left(\frac{z}{L}\right)^2 + \dots \right]. \quad (47)$$

To determine the amplitude  $B$  at leading order in  $\epsilon$  we divide  $\Phi_{\text{mf}}(z)$  by the semi-infinite profile (20) and obtain

$$\frac{\Phi_{\text{mf}}(z)}{\Phi^{[1]}(z)} = \frac{3\pi^2}{2u} [1 + O(u, \epsilon)] \left( \frac{\mu^2 z}{\sqrt{\rho}} \right)^{-\epsilon/2} \left( \frac{z}{L} \right)^2 + \dots \quad (48)$$

At the fixed point  $u_* = (2/3)\epsilon + O(\epsilon^2)$  the amplitude  $B$  is thus given by  $B = 9\pi^2/(4\epsilon) + O(\epsilon^0)$ . Note that  $B$  is of the order  $1/\epsilon$  because the semi-infinite profile vanishes at zero loop order.

### E. Relation to surface critical phenomena in magnetic systems

Recently the crossover between various surface universality classes (special, ordinary, normal) has been studied for systems belonging to the bulk universality class of the Ising model [34]. In this section we briefly discuss the differences and analogies between the surface critical behavior of DDS and the Ising model.

First of all, there is no special point (and no surface transition [11]) in the system studied in the present paper. In Ising systems it is possible that the symmetry is spontaneously broken at the surface (due to enhanced couplings between the surface spins) while the bulk is still in the paramagnetic phase. In DDS, on the other hand, the surface is coupled to a reservoir, which violates particle conservation. As a consequence, the surface cannot order independently from the bulk even if the attractive particle interaction is enhanced near the surface. This will be different for a particle conserving surface parallel to the driving force.

In the semi-infinite  $\phi^4$  model (with zero external field) near the ordinary or special transition there is no coupling between even and odd operators (with respect to reflection,  $\phi \rightarrow -\phi$ ). Therefore the order parameter profile is constant at the ordinary fixed point. As shown above, this is not true for DDS with  $h_1=0$ .

Another difference appears in the distant wall correction. In the  $\phi^4$  model at the normal fixed point the leading term in the SDE of the order parameter field at the surface is not the normal derivative as in Eq. (44) but the stress tensor [30–33]. This gives rise to the well-known  $(z/L)^d$  correction to the order parameter profile.

An especially interesting effect occurs if a small symmetry breaking external surface field is applied to an Ising system (or  $\phi^4$  model) near the ordinary transition. In this case the order parameter profile displays a nonmonotonic crossover to the asymptotic power law  $\sim z^{-\beta/\nu}$  characteristic of the normal fixed point. For small distances  $z$  from the surface the profile is proportional to an increasing power of  $z$  with an exponent that is related to the anomalous dimension  $\eta_1$  of the surface field. This power law may be derived by a SDE for the order parameter [26,34]. Analogously we may expand the profile (35) in powers of  $h_1$  to obtain

$$\Phi(z, h_1) = z^{-\sigma} (a_1 + a_2 h_1 z^{1/\nu_1} + \dots). \quad (49)$$

This expansion suggests a possible way to determine  $\nu_1$  by computer simulations: The difference of two profiles corresponding to different but small values of  $h_1$  is proportional to  $z^{-\sigma+1/\nu_1}$  for  $z \rightarrow 0$ .

## VI. SIMULATION RESULTS

In order to check some of the results presented in the previous section by computer simulations we use the standard Monte Carlo technique with Metropolis spin-exchange jump rates on the two-dimensional, driven Ising lattice gas with attractive interactions [1,2]. The driving force is effectively infinity, i.e., every attempt of a particle to jump in the direction of the driving force is successful unless the jump would violate the excluded volume constraint. Jumps in the direction antiparallel to the driving force have zero probability. We use the critical value of the temperature parameter

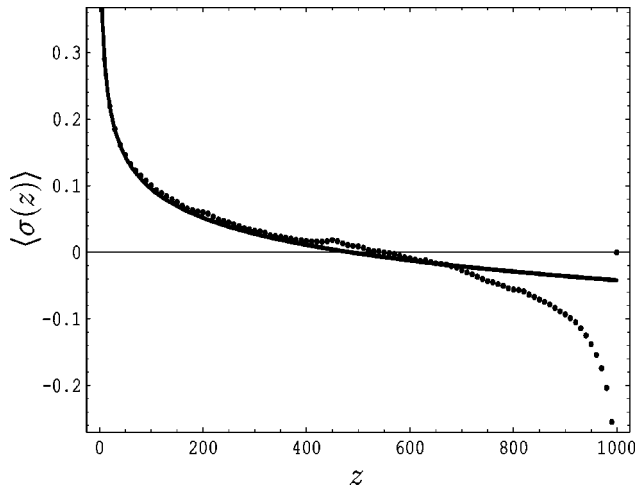


FIG. 3. Density profile for  $c_A=1.0$ ,  $c_B=0.5$ , where the occupation numbers are represented by the spin variable  $\sigma=2n-1$ . The statistical error is everywhere smaller than  $\pm 0.006$ . The solid line is a fit using Eq. (46) with  $A_1=0.678$  and  $B=-1.62$ .

$T_c(\infty)=1.41T_c(0)$  obtained by Leung [2]. The particle reservoirs at the boundaries are incorporated into the model by a simple change of the updating algorithm: Whenever a boundary site is involved in an updating step the occupation number of this site set equal to a random number  $X \in \{0,1\}$  which takes the value 1 with probability  $c_A$  (at the left boundary) or  $c_B$  (at the right boundary). To avoid unwanted correlations each realization of  $X$  has to be used for only one update. In the transverse directions periodic boundary conditions are imposed.

Figure 3 shows the density profile for  $c_A=1.0$  and  $c_B=0.5$ . The system size is  $L_{\parallel}=1000$  in the direction parallel to the driving force and  $L_{\perp}=500$ . At the beginning of each run, an uncorrelated initial state is generated where each lattice site is occupied with probability 0.5. Then  $10^5$  Monte Carlo steps (per site) are performed to reach the stationary state. The profile shown in Fig. 3 has been obtained by averaging over  $2 \times 10^5$  configurations. The amplitudes  $A_1$  and  $B$  in Eq. (46) have been determined by a least square fit with the result  $A_1=0.678 \pm 0.004$ ,  $B=-1.6 \pm 0.2$ . For this fit we have used various subintervals of  $3 \leq z \leq 50$ . (The statistical error in this range is smaller than 0.002.) For larger values of  $z$  higher powers in  $z/L$  become increasingly important. We have checked that the above values for  $A_1$  and  $B$  also provide acceptable fits for smaller systems [ $(L_{\parallel}, L_{\perp})=(500, 397)$  and  $(125, 250)$ ].

To determine the amplitude ratio  $D$  one first has to find the critical value of  $c_A$  that corresponds to a vanishing surface field,  $h_1=0$ . Figure 4 suggests that this value is close to  $c_A \approx 0.28$ . For  $0.278 \leq c_A \leq 0.282$  we obtained fits consistent with  $A_1 = -0.29 \pm 0.02$ . One of these fits is depicted in Fig. 5 together with density profiles for various values of  $c_A$ . Each profile is an average over  $10^6$  configurations. To determine the amplitude  $B$  it would be necessary to obtain a more accurate estimate for the critical surface density. The simulation result for the amplitude ratio reads  $D = -0.43 \pm 0.03$ , which can be compared with our one-loop calculation,  $D \approx -\epsilon/9 = -0.33$  for  $\epsilon=3$ .

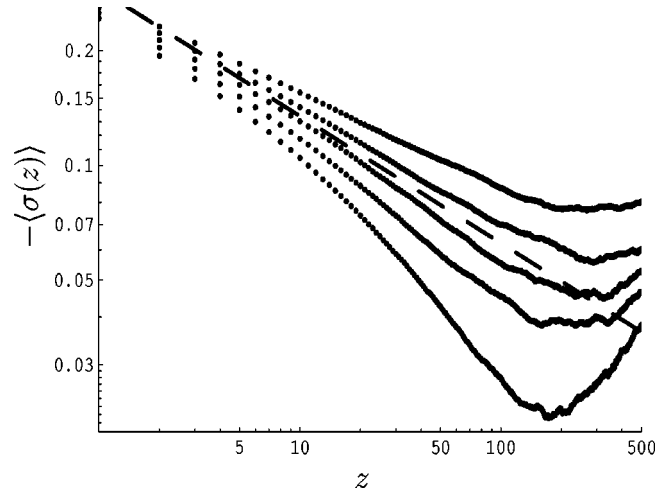


FIG. 4. Double logarithmic plot of the density profile for  $c_A=0.278, 0.280, 0.282, 0.284, 0.286$  (from top to bottom) and  $c_B=0.5$ . The spin variable  $\sigma=2n-1$  has been used. The broken line corresponds to the power  $0.29z^{-1/3}$ .

## VII. SUMMARY AND OUTLOOK

A particle reservoir coupled to the boundary of a driven diffusive system maintains the critical density in the bulk if the chemical potential of the reservoir is not below a critical value. Above this critical value the density profile (as a function of the distance from the boundary) asymptotically approaches the bulk density from above, where the decay of the profile follows a power law with an exponent  $\sigma$ , which can be expressed in terms of the bulk exponent  $\eta$ . At the critical value of the boundary chemical potential the density tends to its bulk value from below. If the chemical potential is close to (but above) its critical value the density profile crosses the critical density at a macroscopic distance  $\zeta$  from the boundary. The singular power law dependence of the length scale  $\zeta$  on the boundary chemical potential is characterized by a new exponent  $\nu_1$ , which has been calculated at first order in  $\epsilon = 5-d$ .

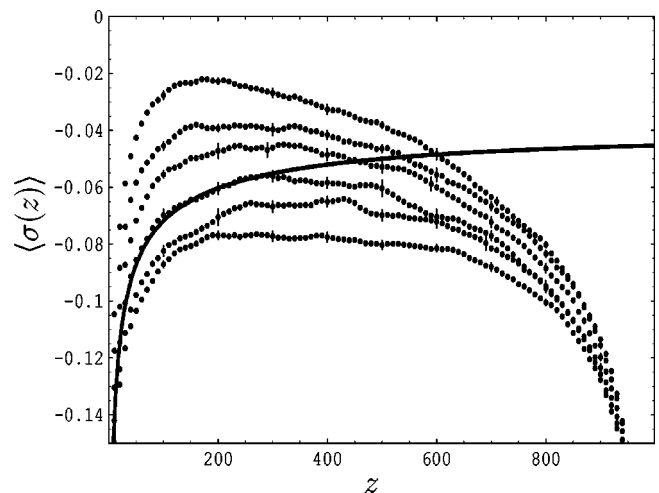


FIG. 5. The density profile for  $c_A=0.278, 0.279, 0.280, 0.282, 0.284, 0.286$  (from bottom to top) and  $c_B=0.5$ . The occupation numbers are represented by the spin variable  $\sigma=2n-1$ . The solid curve is a fit using Eq. (46) with  $A_1=-0.30$  and  $B=0.51$ .

While in exclusion models without particle-particle attraction the density profile is always a monotonic function of the distance from the boundary we have shown that in critical DDS stationary profiles can have local maximum points. This is due to the density correlations in the bulk generated (for  $d > 1$ ) by the attractive interaction. If the “temperature” is raised above  $T_c(E)$  these correlations survive as long as  $T$  is finite. Therefore the *qualitative* form of the density profile will not change for  $T_c(E) < T < \infty$ .

In this paper one out of a multitude of universality classes describing various types of DDS has been considered. These universality classes differ in the nature of the noise (particle conserving or nonconserving), the presence or absence of quenched disorder and the values of temperaturelike critical parameters [35]. We plan to extend the analysis presented here to other universality classes. It is straightforward to derive relations similar to Eq. (36) between  $\sigma$  and the anisotropy exponent  $\eta$  for DDS with quenched disorder. This makes it possible to check the field theoretic predictions of Refs. [36,37,35] for disordered DDS by Monte Carlo simulations of the density profile in systems with open boundaries. Note that in the presence of quenched disorder periodic boundary conditions (in the direction parallel to the driving force) may lead to unwanted correlations since the particles are subjected to the same randomness after every passage through the system.

In order to obtain a numerical estimate for the surface exponent  $\nu_1$  or a more accurate value for the amplitude ratio  $D$  it is necessary to determine the critical surface density more accurately. This is an open problem for future simulations.

#### ACKNOWLEDGMENTS

This work has been supported in part by the Sonderforschungsbereich 237 [Unordnung und Große Fluktuationen

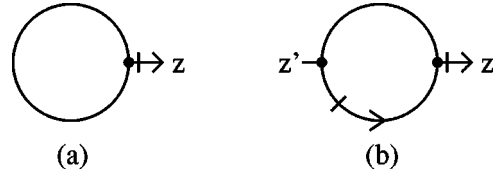


FIG. 6. Ultraviolet divergent Feynman diagrams at one-loop order. A line with (without) an arrow represents the Gaussian propagator (correlator). The short line perpendicular to the propagator line in the diagram (b) indicates a derivative with respect to  $z'$ .

(Disorder and Large Fluctuations)] of the Deutsche Forschungsgemeinschaft.

#### APPENDIX A: SURFACE DIVERGENCES AT ONE-LOOP ORDER

In order to determine the renormalization constants at one-loop order one has to evaluate the ultraviolet divergent Feynman diagrams shown in Fig. 6. The results have to be interpreted in the distribution sense since the calculation of Green functions involves integrations over the  $z$  coordinates of amputated graphs.

The Laplace transform of the first diagram in Fig. 6 reads

$$\begin{aligned} & -\frac{\lambda g}{2} \int_0^\infty dz e^{-sz} \int_{\mathbf{q}_\perp, \omega} \hat{C}_{\mathbf{q}_\perp, \omega}(z, z) \\ & = -\frac{\lambda g}{\epsilon} A_\epsilon \tau^{-\epsilon/2} \left( \frac{\tau^2}{\sqrt{\rho s}} + \frac{4\tau}{3} + \frac{2}{3} \sqrt{\rho s} + O(\epsilon) \right), \end{aligned} \quad (\text{A1})$$

where  $\hat{C}_{\mathbf{q}_\perp, \omega}(z, z)$  is the Gaussian correlator (18) at the Dirichlet fixed point. The two dimensional Laplace transform of the second diagram is given by

$$(\lambda g)^2 \int_0^\infty dz e^{-sz} \int_0^\infty dz' e^{-s'z'} \int_{\mathbf{q}_\perp, \omega} \hat{C}_{-\mathbf{q}_\perp, -\omega}(z, z') \partial_z \hat{G}_{\mathbf{q}_\perp, \omega}(z, z') = \frac{\lambda g^2}{2\sqrt{\rho}\epsilon} A_\epsilon \tau^{-\epsilon/2} \left( \frac{2s'}{s+s'} - \frac{2}{3} + O(\epsilon) \right). \quad (\text{A2})$$

Applying the inverse Laplace transformation to Eqs. (A1) and (A2) we obtain

[Graph 6(a)]

$$= -\frac{\lambda g}{\epsilon} A_\epsilon \tau^{-\epsilon/2} \left( \frac{\tau^2}{\sqrt{\rho}} + \frac{4\tau}{3} \delta(z) + \frac{2}{3} \sqrt{\rho} \delta'(z) + O(\epsilon) \right) \quad (\text{A3})$$

and

[Graph 6(b)]

$$= \frac{\lambda g^2}{2\sqrt{\rho}\epsilon} A_\epsilon \tau^{-\epsilon/2} \left( 2\delta'(z'|z) - \frac{2}{3} \delta(z') \delta(z) + O(\epsilon) \right), \quad (\text{A4})$$

where we have introduced the definition

$$\int_0^\infty dz' \delta'(z'|z) f(z') = -f'(z). \quad (\text{A5})$$

The  $\epsilon$  poles are canceled by the counterterms (25) and (26) given in Sec. V A. The values of the coefficients  $A$ ,  $B$ ,  $F$ ,  $K$ , and  $Z$  at one-loop order follow from Eqs. (A3) and (A4) as

$$A = -\frac{1}{\epsilon}, \quad B = -\frac{u}{3\epsilon}, \quad F = -\frac{4}{3\epsilon}, \quad K = \frac{2}{3\epsilon} \quad (\text{A6})$$

and

$$Z = 1 - \frac{u}{\epsilon}. \quad (\text{A7})$$



- [1] S. Katz, J. L. Lebowitz, and H. Spohn, Phys. Rev. B **28**, 1655 (1983); S. Katz, J. L. Lebowitz, and H. Spohn, J. Stat. Phys. **34**, 497 (1984).
- [2] K.-t. Leung, Phys. Rev. Lett. **66**, 453 (1991).
- [3] H. K. Janssen and B. Schmittmann, Z. Phys. B **64**, 503 (1986).
- [4] B. Schmittmann and R. K. P. Zia, *Phase Transitions and Critical Phenomena*, edited by C. Domb and J. L. Lebowitz (Academic, London, 1995), Vol. 17.
- [5] B. Derrida, E. Domany, and D. Mukamel, J. Stat. Phys. **69**, 667 (1992).
- [6] J. Krug, Phys. Rev. Lett. **67**, 1882 (1991).
- [7] G. Schütz and E. Domany, J. Stat. Phys. **72**, 277 (1993).
- [8] B. Derrida, M. R. Evans, V. Hakim, and V. Pasquier, J. Phys. A **26**, 1493 (1993).
- [9] F. H. L. Essler and V. Rittenberg, J. Phys. A **29**, 3375 (1996).
- [10] D. H. Boal, B. Schmittmann, and R. K. P. Zia, Phys. Rev. A **43**, 5214 (1991).
- [11] H. W. Diehl, in: *Phase Transitions and Critical Phenomena*, edited by C. Domb and J. L. Lebowitz (Academic, London, 1986), Vol. 10, pp. 75–267.
- [12] H. W. Diehl and S. Dietrich, Phys. Lett. **80A**, 408 (1980); H. W. Diehl and S. Dietrich, Z. Phys. B **42**, 65 (1981); Erratum B **43**, 281.
- [13] H. W. Diehl and S. Dietrich, Phys. Rev. B **24**, 2878 (1981).
- [14] H. W. Diehl and S. Dietrich, Z. Phys. B **50**, 117 (1983).
- [15] K. Symanzik, Nucl. Phys. B **190** [FS3], 1 (1981).
- [16] S. Dietrich and H. W. Diehl, Z. Phys. B **51**, 343 (1983).
- [17] H. W. Diehl and H. K. Janssen, Phys. Rev. A **45**, 7145 (1992).
- [18] H. W. Diehl, Phys. Rev. B **49**, 2846 (1994).
- [19] H. K. Janssen and K. Oerding, Phys. Rev. E **53**, 4544 (1996).
- [20] H. K. Janssen, Z. Phys. B **23**, 377 (1976).
- [21] C. De Dominicis, J. Phys. (Paris) Colloq. **37**, C1-247 (1976).
- [22] R. Bausch, H. K. Janssen, and H. Wagner, Z. Phys. B **24**, 113 (1976).
- [23] C. De Dominicis and L. Peliti, Phys. Rev. B **18**, 353 (1978).
- [24] H. K. Janssen, in: *From Phase Transitions to Chaos, Topics in Modern Statistical Physics*, edited by G. Györgyi, I. Kondor, L. Sasvári, and T. Tél (World Scientific, Singapore, 1992), pp. 68–91.
- [25] P. C. Martin, E. D. Siggia, and H. A. Rose, Phys. Rev. A **8**, 423 (1973).
- [26] U. Ritschel and P. Czerner, Phys. Rev. Lett. **77**, 3645 (1996).
- [27] H. W. Diehl, S. Dietrich, and E. Eisenriegler, Phys. Rev. B **27**, 2937 (1983).
- [28] The integral over the gradient  $\partial_{\parallel} \tilde{s}$  (which cancels in a system with periodic boundary conditions) can be written as  $\int_V d^d r \partial_{\parallel} \tilde{s} = \int_{\partial V} d^{d-1} r [\tilde{s}(z \rightarrow \infty) - \tilde{s}_s]$ . Due to particle conservation the contribution  $\tilde{s}(z \rightarrow \infty)$  may not be omitted since response functions with  $q_{\perp} = \omega = 0$  are nonzero for  $z \rightarrow \infty$ .
- [29] M. Benhamou and G. Mahoux, Nucl. Phys. B **305** [FS23], 1 (1988).
- [30] J. L. Cardy, Phys. Rev. Lett. **65**, 1443 (1990).
- [31] E. Eisenriegler, M. Krech, and S. Dietrich, Phys. Rev. Lett. **70**, 619 (1993).
- [32] E. Eisenriegler, *Polymers Near Surfaces* (World Scientific, Singapore, 1993).
- [33] H. W. Diehl, Int. J. Mod. Phys. B **11**, 3503 (1997).
- [34] A. Ciach and U. Ritschel, Nucl. Phys. B **489** [FS], 653 (1997).
- [35] V. Becker, Ph.D. thesis, University of Düsseldorf, 1997 (unpublished).
- [36] V. Becker and H. K. Janssen, Europhys. Lett. **19**, 13 (1992).
- [37] B. Schmittmann and K. E. Bassler, Phys. Rev. Lett. **77**, 3581 (1996).